Applied Surface Science 255 (2009) 6907–6913

Contents lists available at ScienceDirect

Applied Surface Science

journal homepage: www.elsevier.com/locate/apsusc

Effect of titanium powder assisted surface pretreatment process on the nucleation enhancement and surface roughness of ultrananocrystalline diamond thin films

Debabrata Pradhan *, I. Nan Lin

Department of Physics, Tamkang University, Tamsui 251, Taiwan, ROC

ARTICLE INFO

Article history:
Received 11 October 2008
Received in revised form 16 February 2009
Accepted 6 March 2009
Available online 17 March 2009

Keywords:
Diamond nucleation
Microwave plasma CVD
Glancing-incidence XRD
X-ray photoelectron spectroscopy
Atomic force microscopy

ABSTRACT

A superior, easy and single-step titanium (Ti) powder assisted surface pretreatment process is demonstrated to enhance the diamond nucleation density of ultrananocrystalline diamond (UNCD) films. It is suggested that the Ti fragments attach to silicon (Si) surface form bond with carbon at a faster rate and therefore facilitates the diamond nucleation. The formation of smaller diamond clusters with higher nucleation density on Ti mixed nanodiamond powder pretreated Si substrate is found to be the main reason for smooth UNCD film surface in comparison to the conventional surface pretreatment by only nanodiamond powder ultrasonic process. The X-ray photoelectron spectroscopic study ascertains the absence of SiC on the Si surface, which suggests that the pits, defects and Ti fragments on the Si surface are the nucleation centers to diamond crystal formation. The glancing-incidence X-ray diffraction measurements from 100 nm thick UNCD films evidently show reflections from diamond crystal planes, suggesting it to be an alternative powerful technique to identify diamond phase of UNCD thin films in the absence of ultra-violet Raman spectroscopy, near-edge X-ray absorption fine structure and transmission electron microscopy techniques.

© 2009 Elsevier B.V. All rights reserved.

1. Introduction

Diamond thin film is a promising material for a large number of optical, mechanical and electronic applications, such as optical windows [1,2], wear-resistant coatings [3], surface acoustic-wave devices [4], field emission displays [5,6], and heat spreaders [7,8]. However, many existing restrictions hinder the commercial applications of the diamond films, for example: low conductivity, high surface roughness, and high film stress. In the recent years, synthesis of ultrananocrystalline diamond (UNCD) films has improved the structural and tribological characteristics of diamond films to a large extent which obviate many of the limitations just mentioned [9]. The UNCD film is usually deposited by microwave plasma enhanced chemical vapor deposition (MPECVD) using Ar–CH_4 plasma unlike H_2–CH_4 plasma used for producing micro-crystalline diamond films [10]. The UNCD films are normally composed of extremely fine diamond grains (with size 2–10 nm) and therefore possess large area of grain boundaries [10]. The grain boundaries containing non-diamond carbon enhance the electrical properties of UNCD films to manifold, resulting in higher electron field emission, better performance in MEMS and surface acoustic devices [11–15]. In many of these applications, surface roughness needs to be extremely low. The surface roughness of diamond films is directly related to the nucleation density and the grain size. Although, surface roughness is rather low in case of the UNCD films due to its small grain size, there are a few reports for further improving smoothness of the UNCD films by enhancing the nucleation density using special surface pretreatment process [16,17].

Conventionally, Si surface is either mechanically scratched or ultrasonically abraded with diamond powder to create nucleation sites for the diamond nucleation and growth. Single-step seeding technique is also used to grow nanocrystalline diamond thin films [18,19]. In the seeding technique, Si substrates are normally seeded by nanocrystalline diamond powder (with average grains size of 5 nm) using an ultrasonic treatment procedure. This process can increase the seeding density up to 1.0×10^{12} cm^{-2}, which allows growth of ultra-thin fully closed diamond layers [19]. Biased enhanced nucleation is another superior technique to obtain diamond films with a high nucleation density but is limited to conducting substrates. Recently, new nucleation process (NNP) has been developed, which gives ultra-thin, extremely smooth diamond

* Corresponding author. Current address: Department of Chemistry, University of Waterloo, 200 Univ. Avenue West, Waterloo, Ontario, Canada N2L 3G1.
Tel.: +1 519 888 4567x37763; fax: +1 519 746 0435.
E-mail addresses: dpradhan@scimail.uwaterloo.ca (D. Pradhan), inanlin@mail.tku.edu.tw (I.N. Lin).

0169-4332/$ – see front matter © 2009 Elsevier B.V. All rights reserved.
doi:10.1016/j.apsusc.2009.03.013

film with a high diamond nucleation density [17,20,21]. However, the NNP involves two-step process: (1) "plasma treatment"—the substrate needs to be exposed to hydrocarbon plasma to produce a thin layer of hydrogenated amorphous carbon and (2) "seeding step"—substrate has to be taken out of the growth chamber and subjected to ultrasonic treatment in an alcohol solution with diamond nanopowder. To avoid abovementioned time consuming two-step process, Naguib et al. deposited 10 nm thick tungsten layer prior to diamond growth [16]. The tungsten layer significantly increased the diamond nucleation density allowing the formation of a thin UNCD layer (100 nm thick). Moreover, the use of metal particle mixed diamond powder slurry in the ultrasonication process is known to increase the diamond nucleation density in CH_4–H_2 media for the growth of micro-crystalline diamond [22,23]. In the present work, we demonstrate a strong effect of Ti metal mixed nanodiamond (ND) powder surface pretreatment on the diamond nucleation density for the growth of UNCD films and thereby further reducing the surface roughness, without using two-step pretreatment process. This simple and single-step Ti metal mixed nanodiamond (Ti–ND) powder pretreatment process enhances the diamond nucleation density to 10^{12} cm^{-2} and allows to form an ultra-thin UNCD film (100 nm thick) even at a lower substrate temperature (<500 °C) unlike previous two reports which uses higher deposition temperature [16,17]. However, single-step seeding technique has been successfully used to obtain smooth diamond film with high nucleation density at lower deposition temperature (410 °C) [19].

In the present work, atomic force microscope (AFM) is used to measure the surface roughness of fully covered UNCD films. X-ray photoelectron spectroscopy (XPS) is employed to find out the types of bonding and the percentage of carbon accumulation on both the Ti–ND and ND powder pretreated Si surface at a selected deposition time. Furthermore, the large area of grain boundaries containing non-diamond carbon becomes the blocking wall for characterizing the diamond phase of UNCD films with visible Raman spectroscopy. Therefore ultra-violet (UV) Raman spectroscopy and near-edge X-ray absorption fine structure (NEXAFS) techniques are normally used to measure the crystalline quality of UNCD films [24]. Here we demonstrate that the glancing-incidence X-ray diffraction (GIXRD) can be a very useful alternative tool to characterize the diamond phase of UNCD films.

2. Experimental details

One side polished single crystal Si wafers (p-type, boron doped) from Wacker Chemitronic, GmbH, having (1 0 0) crystallographic orientation were used as substrates for UNCD film deposition. At first, Si substrates were thoroughly degreased by sonicating in acetone and isopropyl alcohol, each for 5 min. Then they were subjected to 2 min surface etch in a 40% HF solution to remove the native oxide layer. Subsequently Si substrates were sonicated for 1 h in the slurry of Ti mixed ND powder termed as Ti–ND process. Slurry was prepared in 10 ml methanol by mixing ND powder (particle size—30 nm) with coarse Ti metal particles (size—40 μm) in the weight ratio of 1:1. In another set, slurry was prepared using only ND powder (particle size—30 nm) in methanol termed as ND process. The weight ratio of Ti–ND (200 mg) or ND (200 mg) to methanol (10 ml) was kept constant. After ultrasonication in the

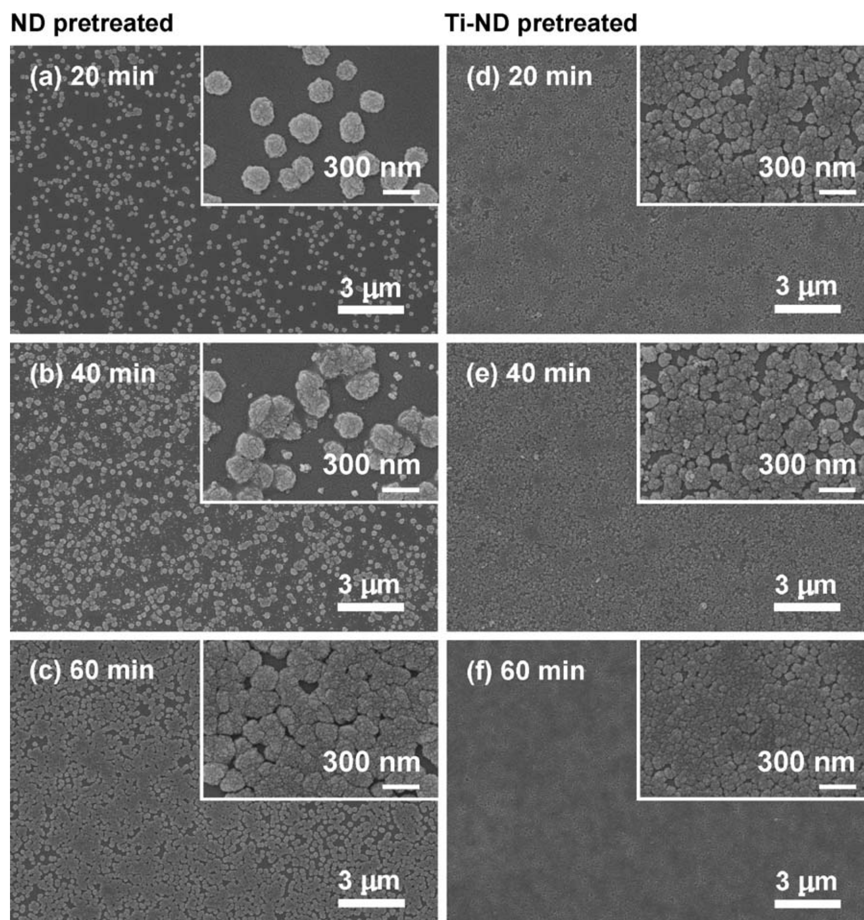

Fig. 1. SEM images of UNCD films deposited for selected time (a–c) on ND pretreated and (d–f) on Ti–ND pretreated Si substrates. Insets show the corresponding magnified images.

Ti–ND or ND powder slurry, Si substrates were thoroughly rinsed in methanol and again ultrasonicated for 5 min in fresh methanol to remove any loose particles sticking to surface. Si substrates were finally dried under nitrogen stream prior to loading for deposition. IPLAS MPECVD system was used for the UNCD film deposition. The UNCD film deposition was carried out as a function of deposition time to observe the nucleation enhancement until Si surface is completely covered by diamond grains. Other detailed deposition conditions were as follows: microwave power—1200 W, CH_4/Ar—1%, flow rate—200 sccm (standard cubic centimeter per minute), chamber pressure—150 Torr, substrate temperature—$\sim$475 °C. The substrate temperature was measured by placing a K-type thermocouple at the bottom surface of molybdenum substrate holder on which Si wafer was kept for deposition. No external heater was used to heat the substrate and the substrate temperature was in between 460 and 475 °C because of Ar–CH_4 plasma heating.

The surface morphologies of diamond films were examined with a field emission scanning electron microscope (FESEM, JSM 6500F). The AFM studies were carried out under ambient condition using a scanning probe microscope (Digital Instruments Nanoscope IV) in non-contact mode using Si tip (tip radius 5–10 nm). The XPS spectra were collected with Perkin-Elmer PHI1600ESCA System using MgK_{α} X-ray source (1253.6 eV). Raman spectra of UNCD films were recorded with a Renishaw Raman spectrophotometer using an excitation wave length of 514 nm obtained by Ar laser. The GIXRD patterns of the samples were recorded in a PANalytical X-ray diffractometer using Cu K_{α} line at an incident angle of 0.3° from a X-ray generator operated at 40 kV and 40 mA.

3. Results and discussion

3.1. Morphology study

Fig. 1 shows the morphologies of UNCD films on Si substrates pretreated by either ND (Fig. 1a–c) or Ti–ND (Fig. 1d–f) process. The insets of Fig. 1 show the corresponding magnified SEM images. As anticipated, the diamond nucleation density is found to increase continually with deposition time. There are a few clusters of diamond grains after 20 min of deposition on ND pretreated Si (Fig. 1a), whereas at the same deposition time, a large area of substrate is covered by diamond grains on Ti–ND pretreated Si (Fig. 1b). Similar drastic enhancement in the diamond nucleation density is evident on Ti–ND pretreated substrates at a deposition time of 40 min (Fig. 1e) and 60 min (Fig. 1f) as compared to the ND pretreated substrates. The main reason of higher diamond nucleation density on Ti–ND pretreated substrates is obviously due to the effect of Ti metal. To verify whether the effect of diamond nucleation density is due to only Ti metal, we deposited UNCD film for 60 min on Si substrate pretreated with only Ti powder (without mixing ND powder in it). However, the nucleation density on only Ti pretreated Si substrate was found to be even smaller (image not shown) than that obtained by ND process. This suggests the need of both ND and Ti powder to achieve the higher diamond nucleation density. The diamond nucleation is known to occur at the defects and pits on the substrate created either by diamond powder scratching or by ultrasonication [25]. When ultrasonication is carried out using Ti–ND powder, ND powder creates pits and defects on the surface and it is believed that the Ti fragments adhered to those finely damaged sites or pits. As Ti is one of the best carbide forming metal and has higher solubility with carbon in comparison to Si, Ti has greater possibility of forming bond with carbon and thereby nucleate diamond at a shorter deposition time. It should also be noted that the diffusivity of carbon species in Ti [$(D_c)_{Ti} = 7 \times 10^{-9}$ cm^2/s] is about six orders of magnitude higher than that of the carbon in Si [$(D_c)_{Si} = 2.0 \times 10^{-15}$ cm^2/s] [25]. Therefore, it is apparent why there has been a higher diamond nucleation density on Ti–ND pretreated substrates. Furthermore, the bright dots in the magnified SEM image (shown in the inset of Fig. 1a) are cauliflower shaped cluster of diamond made up of very fine grains of size less than 10 nm. The unique property of CH_4–Ar plasma is known to produce uniform UNCD crystals (<10 nm in size) without increasing the crystal size as it happens in the case of microcrystalline diamond growth in the H_2 rich plasma. At the early growth stage of UNCD film, fine diamond crystal begins to grow from the high energetic nucleation sites (i.e. pits, defects and Ti fragments) of the substrate. Eventually secondary nucleation takes place on each diamond grain and more number of diamond grains grow on the exposed surface of each diamond grain forming cluster [26,27]. The size of cauliflower-like clusters continues to increase three dimensionally with increase in the deposition time until they coalesce. After 20 min of deposition, the average size of clusters formed on the substrate pretreated with ND and Ti–ND process was 120 nm (Fig. 1a) and 60 nm (Fig. 1d), respectively. The formation of smaller clusters with a higher diamond nucleation density on Ti–ND pretreated substrate therefore makes it an ideal pretreatment approach to deposit UNCD films.

Fig. 2a and b shows the morphology of fully UNCD covered Si surface deposited for 90 min on ND and Ti–ND pretreated substrates, respectively. It takes 90 min to obtain a continuous UNCD film (nucleation density—10^{12} cm^{-2}) on ND pretreated substrate whereas continuous UNCD film with a very few voids is

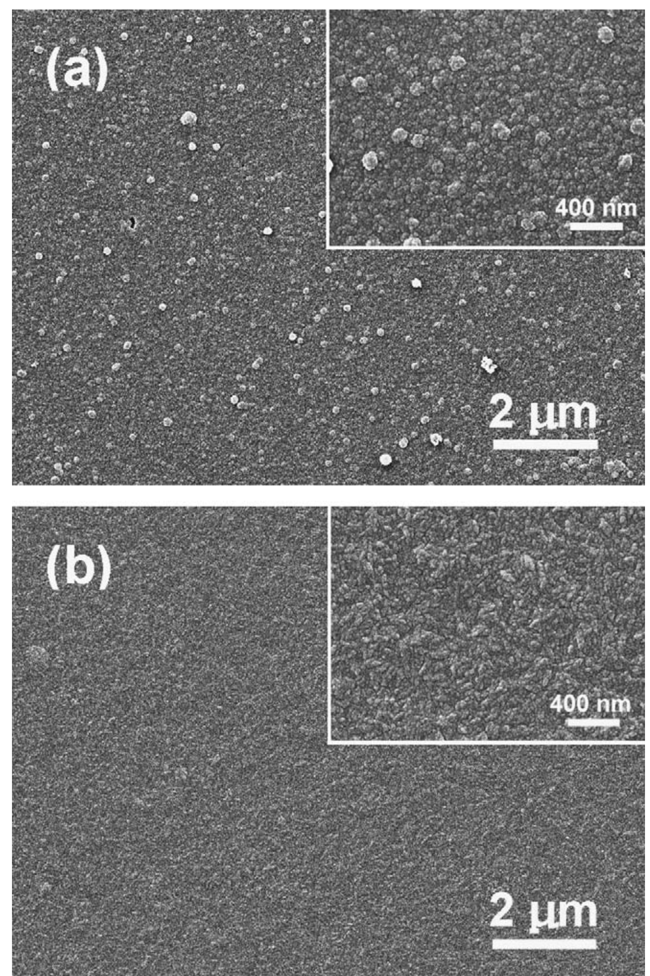

Fig. 2. The SEM images of UNCD films deposited for 90 min on (a) ND and (b) Ti–ND pretreated Si substrates. The insets show corresponding magnified images.

obtained after 60 min deposition on Ti–ND pretreated substrate (Fig. 1f). In addition, a higher surface roughness of UNCD film is evident on ND pretreated substrate (Fig. 2a) in comparison to Ti–ND pretreated substrate (Fig. 2b). The thickness of fully covered UNCD film deposited for 90 min was measured to be 100 nm from the cross-sectional SEM image (not shown). There was no change in the thickness of UNCD films on differently pretreated substrates suggesting growth rate is independent to pretreatment process. It is worth to note that, film deposition in the present work was carried out at a low substrate temperature (∼475 °C). It is well known that the nucleation and growth rate is poor at lower substrate temperature as compared to high temperature deposition [28,29]. Therefore, a continuous UNCD film can be obtained at much shorter deposition time at high substrate temperature. Moreover, seeding technique has been successfully used to obtain smooth nanocrystalline diamond films even at lower deposition temperature (410 °C) because it does not need initial nucleation [19].

3.2. Atomic force microscopy of UNCD films

Fig. 3(a, b) and (c, d) shows the surface topologies of UNCD films deposited on the Si substrates for 90 and 180 min, respectively, pretreated with ND (Fig. 3a and c) and Ti–ND (Fig. 3b and d) process. While shorter deposition time (90 min) presents the surface topology at the time UNCD clusters coalesce to form a film (with thickness of 100 nm), a longer deposition time (180 min) displays the surface topology of a thicker UNCD film (with thickness ∼500 nm). Table 1 lists the root mean square (RMS) roughness of UNCD films deposited on ND and Ti–ND pretreated substrates at various scan ranges. The RMS roughness of UNCD films deposited for either 90 or 180 min on Ti–ND pretreated substrates was found to be smaller than that of ND pretreated substrates at any given scan range. The smaller surface roughness of UNCD film on Ti–ND pretreated substrates is mainly due to the formation of smaller clusters with higher diamond nucleation density (apparent in Fig. 3b and d) and are also in good accord with SEM images (Fig. 1d–f). This suggests that the secondary nucleation and growth is depended on the initial growth topology. However, the RMS roughness is found to increase for a thicker UNCD film deposited for 180 min on both the ND and Ti–ND pretreated substrates. Similar observation in the increase of surface roughness with deposition time has been reported by Kromka et al. [19]. The increase in the surface roughness after 180 min of deposition appears to be due to the increase in individual cauliflower-like cluster size. Moreover, there is almost 30% reduction in the surface roughness of UNCD films deposited on Ti–ND pretreated Si substrates as compared to ND pretreated substrates. This demonstrates that Ti–ND pretreatment process is superior to ND pretreatment process for the deposition of UNCD films with a higher diamond nucleation density. Although the surface roughness of UNCD film (7.86 nm, over a 1 μm^2 area) on Ti–ND pretreated Si is higher than that of modified NNP (3.3 nm over a 1 μm^2 area, deposition temperature 750 °C), it should be noted that the deposition in the present work is carried out at a lower substrate temperature (475 °C). Furthermore, present surface pretreatment has certain advantages because of single-step conventional ultrasonication unlike NNP or use of tungsten intermediate layer for UNCD growth, both of which use two-step pretreatment process [16,17].

3.3. X-ray photoelectron spectroscopy of UNCD films

XPS is an important technique to understand the nucleation behavior of diamond on the Si surface. Several literatures have reported not only the formation of SiC layer but also its thickness is crucial to the nucleation of micro-crystalline diamond [30–32]. However, there are a limited number of XPS studies carried out on the nucleation of UNCD films [17]. To understand the nucleation and growth of UNCD films, XPS analysis was carried out on pretreated Si surface and UNCD films deposited for selected time (20, 40, 60 and 90 min). Fig. 4 shows a typical XPS survey spectrum

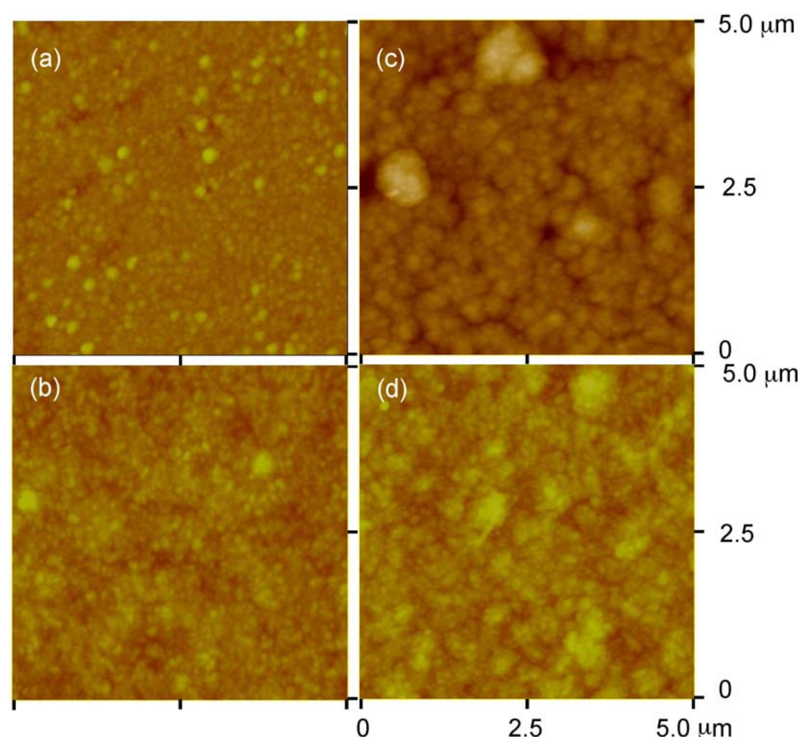

Fig. 3. AFM images of UNCD films deposited for 90 min (a and b) and 180 min (c and d) on ND (a and c), and Ti–ND (b and d) pretreated Si substrates.

Table 1
Room mean square (RMS) surface roughness of UNCD films deposited for 90 and 180 min on ND and Ti–ND pretreated Si substrates.

Pretreatment process	Scan range	RMS roughness after 90 min	RMS roughness after 180 min
ND pretreated	1 μm × 1 μm	11.27 nm	11.34 nm
	5 μm × 5 μm	13.7 nm	25.18 nm
TiND pretreated	1 μm × 1 μm	7.86 nm	9.12 nm
	5 μm × 5 μm	10.24 nm	17.0 nm

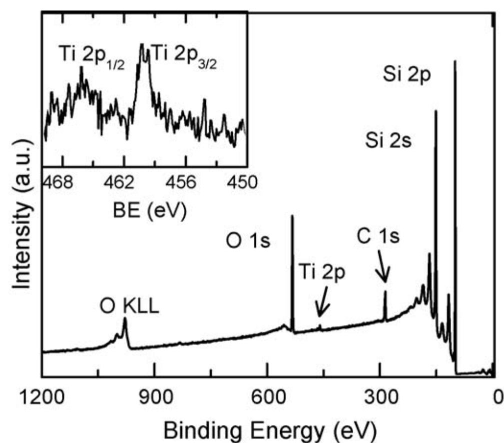

Fig. 4. XPS survey spectrum from a Ti–ND pretreated Si substrate prior to UNCD deposition. The inset shows the Ti 2p region spectrum.

obtained from Si surface, which was ultrasonically pretreated with Ti mixed ND powder (Ti–ND process). In addition to prominent XPS peak of Si 2p at 99.7 eV, C 1s at 285.5 eV and O 1s at 533.0 eV, a smaller (minor) peak for Ti 2p is observed at 459.6 eV. The inset of Fig. 4 shows the region spectrum for Ti 2p. Interestingly, the Ti on the pretreated Si surface is found to be in the oxide form (TiO_2) rather than in its metallic form taken in the beginning for ultrasonication. It is believed that the small quantity of Ti fragments attached on the Si surface is converted to TiO_2 upon being exposed to the environment. However, the high diamond nucleation density observed on Ti–ND pretreated substrates clearly suggests the effect of Ti on silicon surface despite being converted to TiO_2 phase.

Fig. 5a and b shows the C 1s photo peak of XPS spectra collected from UNCD films deposited for selected time on ND and Ti–ND pretreated substrates, respectively. The broad C 1s peak at ~285.5 eV confirms the substantial quantity of sp^3 carbon in the UNCD films, in accordance with the literature binding energy (BE) value of 284.3 and 285.2 eV for sp^2 and sp^3 hybridized carbon atoms, respectively [33,34]. Two important changes in the C 1s signal is noticed from the UNCD films deposited for selected deposition time. First, there is a higher BE shift of C 1s peak with increase in the deposition time [285.3 eV (285.5 eV) and 285.5 eV (285.7 eV) for 20 and 90 min UNCD deposition on ND (Ti–ND) pretreated substrate, respectively], suggesting increase of the sp^3 character in the UNCD films. The lower BE position for C 1s after initial UNCD depositions (20 and 40 min) is believed to be due to some graphitic or amorphous carbon formation on the Si surface prior to the UNCD growth. Lifshitz et al. have previously reported the formation of amorphous carbon layer on the Si surface prior to growth of diamond crystal [35]. Second, the increase of C 1s peak intensity (counts per second) with UNCD deposition time is obviously due to increase in the density of diamond grains on the Si substrates. It is important to note that there are no SiC features in our XPS spectra from the UNCD films obtained at any deposition time, which supports the findings of Lee et al. that SiC formation must not be the only criterion for diamond nucleation [36]. However, formation of SiC in the previous reports is most possibly due to the biased enhanced growth. In the biased enhanced growth, energetic ions and methyl radicals forcefully bombarded to Si substrate that led to the formation of a SiC layer prior to diamond growth [30]. Recently, Sumant et al. also revealed the formation SiC along with a layer of ultra-thin, hydrogenated, amorphous carbon on the substrate in their first step surface plasma treatment for the growth of UNCD films [17]. This suggests that formation of SiC is very sensitive to the deposition conditions.

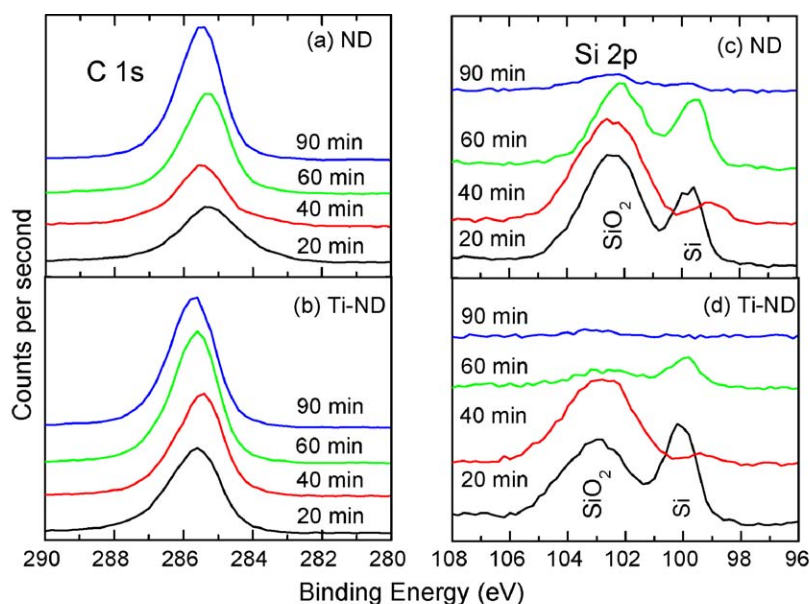

Fig. 5. XPS spectra of (a and b) C 1s and (c and d) Si 2p regions for UNCD films deposited on (a and c) ND pretreated and (b and d) Ti–ND pretreated Si substrates.

In the present work, the absence of SiC indicates that the defects and pits formed on the Si surface during ultrasonic agitation could be the centers to diamond nucleation. Furthermore, neither Ti nor TiC features are observed in the XPS spectra from UNCD films deposited on Si substrates pretreated by Ti–ND process. This could be due to a very minute quantity of Ti fragments on Si surface (as observed in Fig. 4) that has no sufficient sensitivity to be detected by XPS after being covered by UNCD clusters or film. Fig. 5c and d shows the Si 2p region of the XPS spectra obtained from UNCD films deposited on Si substrates pretreated by ND and Ti–ND process, respectively. For shorter deposition time (20 and 40 min), Si 2p photo peak of elemental Si at 99.0 eV and SiO_2 at 103.0 eV is prominent [37]. The presence of SiO_2 is due the post-formation of oxide on the exposed Si surface. The XPS spectra of Si 2p region additionally confirm the absence of SiC (Si 2p peak for SiC is normally observed at 98.8–99.5 eV) [37]. The decrease in the intensity of Si 2p feature with increase in the UNCD film deposition time is due to higher surface coverage of diamond grains. Evidently, Si 2p features from UNCD film deposited for 60 min on Ti–ND pretreated substrate is almost flattened whereas same is prominent from UNCD film deposited on ND pretreated substrate. This further suggests the higher surface coverage of diamond grains on Ti–ND pretreated substrate.

Fig. 6a and b shows the change in atomic percentage of carbon (C), Si and oxygen (O) as a function of UNCD film deposition time on ND and Ti–ND pretreated substrates, respectively. A sharp increase in the C percentage of UNCD films is observed when deposition time increases from 40 to 60 min. This is due to coalesce of diamond clusters to form a film as shown in the SEM images (Fig. 1). The increase of C percentage even after 60 min of deposition on the ND pretreated substrate is due to the incomplete coverage of diamond grains on the surface. Nevertheless, the C percentage remains almost constant after 60 min deposition on Ti–ND pretreated substrate suggesting complete surface coverage at 60 min deposition.

3.4. Raman spectroscopy of UNCD films

Fig. 7a and b shows the typical Raman spectra of continuous UNCD films deposited on ND and Ti–ND pretreated Si substrates, respectively. As UNCD film possesses very fine diamond grains, the non-diamond (or graphitic) carbon present in the grain boundaries significantly contributes towards the Raman spectrum and therefore no sharp peak is observed. Normally four major Raman features at ~1140–1180, ~1350, ~1470 and ~1580 cm^{-1} are obtained from UNCD film [22,38]. The curve in the present Raman spectra is well matched to the reported literatures [24,38]. The prominent bands at ~1340 and ~1550 cm^{-1} are designated as D-band and G-band, respectively, which are due to disorderliness of carbon phase present in the grain boundaries of UNCD films. Absence of sharp feature at 1332 cm^{-1} is due to very small size diamond grains ($\leq$ 10 nm) in the UNCD film and the use of visible Raman spectrometer, which is more sensitive towards sp^2 and amorphous carbon. Nonetheless, same type of UNCD films show sharp feature at 1332 cm^{-1} by UV Raman spectroscopy [24]. The other Raman features that observed from the present UNCD films are at ~1180 and ~1470 cm^{-1} (not prominent because of broad G-band). Ferrari and Robertson have assigned these two features at ~1180 and ~1480 cm^{-1} to C=C bond stretching vibration (ν_1) and C–C bond stretching vibration (ν_3), respectively, of transpolyacetylene segments present at the grain boundaries and surfaces of diamond film [39]. Recently, Kuzmany et al. have given stronger evidence that the peaks at ~1180 and ~1470 cm^{-1} do not originate from the diamond or sp^3 phase of carbon [38]. These two peaks are more distinct in the UNCD films indicating grain boundaries containing transpolyacetylene.

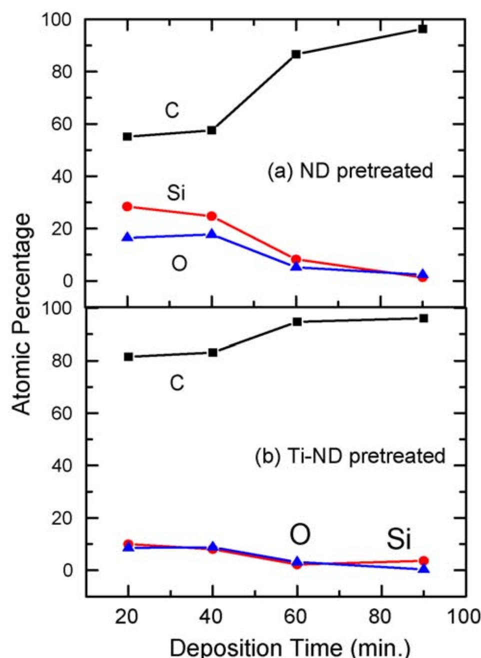

Fig. 6. Atomic percentage C, Si and O of UNCD films deposited on (a) ND and (b) Ti–ND pretreated Si substrates as a function of deposition time.

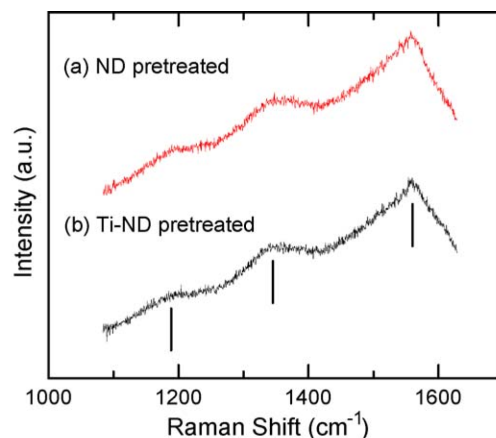

Fig. 7. Raman spectra of UNCD films deposited on (a) ND and (b) Ti–ND pretreated substrates.

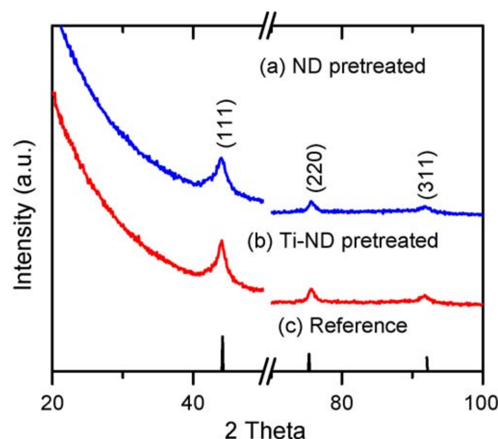

Fig. 8. GIXRD spectra of UNCD films deposited on (a) ND, (b) Ti–ND pretreated substrates along with (c) bar chart of the reference single crystal diamond (JCPDS 00-001-1249).

3.5. Glancing-incidence X-ray diffraction of UNCD films

The visible Raman spectroscopy becomes a bottleneck to interpret UNCD films because of its high sensitiveness towards sp^2 bonded carbon. Although conventional XRD has been successfully used to confirm diamond phase, it becomes poorly sensitive to detect diamond phase in the UNCD thin films [40]. In the present work, we demonstrate that GIXRD is a powerful alternative technique (in the absence of UV Raman) to ascertain the diamond phase in the UNCD films. Fig. 8a and b shows the GIXRD spectra of UNCD films (with thickness 100 nm) deposited on ND and Ti–ND pretreated Si substrates, respectively. Both the UNCD films show identical GIXRD patterns with diffraction features located at 43.98°, 75.53°, and 91.76°, corresponding to the (1 1 1), (2 2 0), and (3 1 1) planes, respectively, in good accord with reference single crystal diamond (JCPDS 00-001-1249) [41]. Furthermore, using the Scherrer formula [applied to the (1 1 1) diffraction feature] the approximate diamond grain size was calculated to be 7 and 9.5 nm for UNCD films deposited on ND and Ti–ND pretreated substrates, respectively. The instrumental peak broadening was subtracted after background correction of (1 1 1) feature for the full-width-half-maximum used in the Scherrer formula. There were no XRD features from graphite or amorphous carbon confirming that the UNCD films obtained in the present work are mainly composed of diamond grains and are crystalline in nature.

4. Conclusions

The present work demonstrates the superiority of ultrasonic pretreatment using Ti–ND powder in comparison to that of only ND powder. The formation of smaller cauliflower-like diamond clusters with a higher nucleation density on Ti–ND pretreated substrates allow faster conglomeration of clusters to form UNCD film with a smaller surface roughness as confirmed by SEM and AFM. The XPS measurements on the UNCD films deposited for selected deposition time show primarily sp^3 bonded carbon. The absence of SiC features clearly suggests that the diamond nucleation occurred on defects and pits formed during ultrasonication and on Ti fragments (even though Ti is converted to oxide form) attached to the Si surface on Ti–ND pretreated substrates. The lower BE position of C 1s XPS feature from the UNCD films deposited for shorter time (20 and 40 min) is believed to be due to graphitic or amorphous carbon formation on the Si surface prior to UNCD growth. The typical visible Raman spectra of UNCD films show the D-band, G-band and transpolyacetylene segments of disorder carbon. The GIXRD spectra ascertain the diamond phase in the UNCD films with a grain size of 7–9 nm.

Acknowledgement

Authors are thankful to Prof. K.T. Leung, University of Waterloo, for allowing the WATLab facilities for characterizing UNCD films by GIXRD and AFM.

References

[1] K. Meykens, K. Haenen, M. Nesladek, L.M. Stals, C.S.J. Pickles, R.S. Sussmann, Diam. Relat. Mater. 9 (2000) 1021.
[2] Y. Kawano, S. Chiba, A. Inoue, Rev. Sci. Instrum. 75 (2004) 279.
[3] J. Li, Q. Zhang, S.F. Yoon, J. Ahn, Q. Zhou, S. Wang, D. Yang, Q. Wang, Z. Li, J. Wang, Q. Lei, J. Appl. Phys. 92 (2002) 6275.
[4] M.B. Assouar, O. Elmazria, P. Kirsch, P. Alnot, V. Mortet, C. Tiusan, J. Appl. Phys. 101 (2007) 114507.
[5] O. Ternyak, R. Akhvlediani, A. Hoffman, W.K. Wong, S.T. Lee, Y. Lifshitz, S. Daren, E. Cheifetz, J. Appl. Phys. 98 (2005) 123522.
[6] K. Subramanian, W.P. Kang, J.L. Davidson, J. Vac. Sci. Technol. B 25 (2007) 532.
[7] G.B. Kim, J.-Y. Kim, J. Lee, J. Yoo, K.-S. Kim, S.-M. Lee, S. Cho, S.-J. Lim, T. Kim, Y. Park, Appl. Phys. Lett. 89 (2006) 181106.
[8] J.-Y. Kim, S. Cho, S.-M. Lee, G.B. Kim, J. Lee, J. Yoo, K.-S. Kim, T. Kim, Y. Park, Electron. Lett. 43 (2007) 105.
[9] J.A. Carlisle, O. Auciello, Electrochem. Soc. Interface 12 (2003) 28.
[10] S. Jiao, A. Sumant, M.A. Kirk, D.M. Gruen, A.R. Krauss, O. Auciello, J. Appl. Phys. 90 (2001) 118.
[11] W. Zhu, G.P. Kochanski, S. Jin, Science 282 (1998) 1471.
[12] A.R. Krauss, O. Auciello, M.Q. Ding, D.M. Gruen, Y. Huang, V.V. Zhirnov, E.I. Givargizov, A. Breskin, R. Chechen, E. Shefer, V. Konov, S. Pimenov, A. Karabutov, A. Rakhimov, N. Suetin, J. Appl. Phys. 89 (2001) 2958.
[13] S. Srinivasan, J. Hiller, B. Kabius, O. Auciello, Appl. Phys. Lett. 90 (2007) 134101.
[14] B. Bi, B. Golding, W.S. Huang, J. Asmussen, US Patent 6,858,969 (2005).
[15] C.-H. Chou, Y.-C. Lin, J.-H. Huang, N.H. Tai, I.-N. Lin, Diam. Relat. Mater. 15 (2006) 404.
[16] N.N. Naguib, J.W. Elam, J. Birrell, J. Wang, D.S. Grierson, B. Kabius, J.M. Hiller, A.V. Sumant, R.W. Carpick, O. Auciello, J.A. Carlisle, Chem. Phys. Lett. 430 (2006) 345.
[17] A.V. Sumant, P.U.P.A. Gilbert, D.S. Grierson, A.R. Konicek, M. Abrecht, J.E. Butler, T. Feygelson, S.S. Rotter, R.W. Carpick, Diam. Relat. Mater. 16 (2007) 718.
[18] I.B. Yanchuk, M.Ya. Valakh, A.Ya. Vul, V.G. Golubev, S.A. Grudinkin, N.A. Feoktistov, A. Richter, B. Wolf, Diam. Relat. Mater. 13 (2004) 266.
[19] A. Kromka, Š. Potocký, J. Čermák, B. Rezek, J. Potměšil, J. Zemek, M. Vaněček, Diam. Relat. Mater. 17 (2008) 1252.
[20] T.H. Metcalf, X. Liu, B.H. Houston, J.W. Baldwin, J.E. Butler, T. Feygelson, Appl. Phys. Lett. 86 (2005) 81910.
[21] S. Rotter, in: M. Yoshikawa, Y. Koga, Y. Tzeng, C.-P. Klages, K. Miyoshi (Eds.), Proceedings of the Applied Diamond Conference/Frontier Carbon Technologies, ADC/FCT'99, vol. 25, MYU K.K., Tokyo, 1999.
[22] Y. Chakk, R. Brener, A. Hoffman, Appl. Phys. Lett. 66 (1995) 2819.
[23] E.R. Shima, I. Gouzman, M. Folman, A. Hoffman, S. Rotter, Diam. Relat. Mater. 8 (1999) 139.
[24] X. Xiao, J. Birrell, J.E. Gerbi, O. Auciello, J.A. Carlisle, J. Appl. Phys. 96 (2004) 2232.
[25] H. Liu, D.S. Dandy, Diam. Relat. Mater. 4 (1995) 1173.
[26] J. Birrell, J.A. Carlisle, O. Auciello, D.M. Gruen, J.M. Gibson, Appl. Phys. Lett. 81 (2002) 2235.
[27] Y. Lifshitz, C.H. Lee, Y. Wu, W.J. Zhang, I. Bello, S.T. Lee, Appl. Phys. Lett. 88 (2006) 243114.
[28] P. Reinke, P. Kania, P. Oelhafen, R. Guggenheim, Appl. Phys. Lett. 68 (1996) 22.
[29] W. Kulisch, C. Popov, S. Boychev, M. Jelinek, P.N. Gibson, V. Vorlicek, Surf. Coat. Technol. 200 (2006) 4731.
[30] B.R. Stoner, G.H.M. Ma, S.D. Wolter, J.T. Glass, Phys. Rev. B 45 (1992) 11067.
[31] D.N. Belton, S.J. Harris, S.J. Schmieg, A.M. Weiner, T.A. Perry, Appl. Phys. Lett. 54 (1989) 416.
[32] S.D. Wolter, J.T. Glass, B.R. Stoner, J. Appl. Phys. 77 (1995) 5119.
[33] P. Merel, M. Tabbal, M. Chaker, S. Moisa, J. Margot, Appl. Surf. Sci. 136 (1998) 105.
[34] J. Diaz, G. Paolicelli, S. Ferrer, F. Comin, Phys. Rev. B 54 (1996) 8064.
[35] Y. Lifshitz, X.M. Meng, S.T. Lee, R. Akhveldiany, A. Hoffman, Phys. Rev. Lett. 93 (2004) 56101.
[36] S.T. Lee, H.Y. Peng, X.T. Zhou, N. Wang, C.S. Lee, I. Bello, Y. Lifshitz, Science 287 (2000) 104.
[37] J.F. Moulder, W.F. Stickle, P.E. Sobol, K.D. Bomben, in: J. Chastain (Ed.), Handbook of X-ray Photoelectron Spectroscopy, PerkinElmer Corporation, MN, USA, 1992.
[38] H. Kuzmany, R. Pfeiffer, N. Salk, B. Gunther, Carbon 42 (2004) 911.
[39] A.C. Ferrari, J. Robertson, Phys. Rev. B 63 (2001) 121405.
[40] L.-J. Chen, N.-H. Tai, C.-Y. Lee, I.-N. Lin, J. Appl. Phys. 101 (2007) 064308.
[41] PDF-2 Database, International Center for Diffraction Data (ICDD), 2004.